

Fingerprints of a Classical Resonance on the Eigenlevel Dynamics of the Corresponding Quantum Hamiltonian[†]

Srihari Keshavamurthy

Department of Chemistry, Indian Institute of Technology, Kanpur U. P. 208 016, India

Received: September 19, 2000

The dynamics of the energy eigenvalues of a single resonance, two-mode quantum Hamiltonian with varying resonance coupling is studied. The resonant quantum states are linked to straight-line parametric level motion in the level dynamics. On the basis of the analogy to the periodic orbit scarring of eigenstates giving rise to linear parametric level motion, we suggest that the resonant states give rise to such soliton-like features in the level dynamics. As a result, resonant states for a given polyad constitute a solitonic “fan” structure manifesting throughout the energy regime. Isomorphic fans, at specific polyad intervals, are identified for which the level velocities of the corresponding states are related by a translation along the classical resonance line. An analysis of the level velocities for isomorphic states indicates that the level velocities of a $m:n$ resonant state beyond a certain critical coupling strength scale with the polyad P as $P^{(m+n)/2}$. Numerical studies on a 1:1 resonant system confirm the expected scaling and suggest $(P - 2\nu)$ as the asymptotic velocity of a state $|P;\nu\rangle$, where ν is the degree of excitation of the state. Persistence of the fan structure on the addition of another independent resonance leads to the possibility of understanding and assigning highly excited states via the scars of the independent resonances.

Introduction

Classical-quantum correspondence for resonant systems has been an area of considerable interest for quite some time and continues to attract attention from the chemical physics community.^{1–4} One of the main motivations for such efforts, apart from the fundamental nature of the problem and the ubiquity of resonances in physical phenomena,⁵ is the fact that effective resonant Hamiltonians arise naturally in the attempts to understand the spectra of highly excited polyatomic molecules.^{3,6} The dynamics of highly vibrationally excited molecules is very different as compared to the dynamics at low energies due to the pronounced manifestation of the anharmonicities. At such high levels of excitation, the usual low-energy description⁶ based on harmonic, noninteracting normal modes is too simplistic. For example, recent studies⁷ on the bending dynamics of C₂H₂ at around 15 000 cm^{−1} of internal energy reveals local bend and counter-rotation modes which are unrelated to the low energy normal trans and cis bend motions. The marked change in the dynamics happens at energies where zeroth-order normal modes begin to interact strongly, mediated by nonlinear resonances arising from the anharmonicities of the potential. For instance, large amplitude bending motion in the HCP molecule have been identified experimentally,^{8,9} which arise due to a 1:2 Fermi resonance between the bending and the CP stretching motions at about 13 800 cm^{−1} above the ground state.¹⁰ Modes interacting resonantly can exchange energy, and the presence of many such resonances between the various modes in a molecule leads to the phenomenon of intramolecular vibrational energy redistribution (IVR).^{11–13} The resulting complicated spectrum has encoded in it the signatures of the various resonances present in the system. In this sense, resonances and energy flow are synonymous—the presence of

one implies the existence of the other. Thus, given the key role played by resonances in determining the nature of the chemical reactions, it is not surprising that they are crucial for analyzing the spectra of highly excited molecules.^{14,15}

It is clear that rationalizing and, hence, assigning the spectral features of highly excited molecules require a detailed understanding of the nature of the eigenstates and eigenvalues of the resonant system. From a theoretical standpoint, a promising approach is to study the classical, semiclassical, and quantum dynamics of the resonant Hamiltonians. This is evident from the numerous recent studies^{7,10,16,17} on small polyatomics. The advantage of such a classical-quantum correspondence-based approach is that the various dynamical routes to IVR can be identified. A dynamical assignment can then be provided for the states which offers the possibilities of exploiting potential mode specific reaction pathways.

The majority of the work done from a classical-quantum correspondence perspective can be broadly classified into two main approaches. One approach is to explore the consequences of the classical resonance on the eigenvalue spectrum,^{18–33} and the second pertains to the signatures of the underlying resonances manifesting in the eigenstates of the system.^{7,10,16,17,35–37} As far as the latter approach is concerned, it has been shown that a knowledge of the phase space structure of the classical limit resonant Hamiltonian in terms of the periodic orbits,^{7,10,17} resonance zones,^{16,38,43} and higher-dimensional tori is central to our ability to assign the quantum states. Enormous progress has been made in the case of single-resonance Hamiltonians.^{44–52} For example, in such instances, determination of the periodic orbits and their bifurcation structure^{44–48} allows one to classify the eigenstates according to the underlying classical dynamics. Certain special multimode, multiresonant systems which possess enough time-independent constants of the motion, i.e., polyads^{53,54} can also be usefully analyzed from the periodic orbit

[†] Part of the special issue “William H. Miller Festschrift”.

perspective.^{7,55,56} However, two important observations are that the required number of polyads might not always exist and periodic orbits are not sufficient in many instances¹⁶ for understanding the eigenstates. In addition, a significant limitation comes from the fact that detailed knowledge of the phase space structure of three or higher degrees of freedom resonant Hamiltonians is very sparse.⁵⁷ Even if one has the phase space structure at hand, techniques such as comparing the surface of section with the Husimi function⁵⁸ of a given eigenstate become very difficult to implement. In this paper, the focus is on the former approach, which involves identifying the fingerprints of the various resonances on the eigenenergy spectrum.

A number of researchers have investigated^{18–22} the effect of resonances on the energy levels of fixed Hamiltonians. Here, one studies the system for a fixed value of the coupling strength and varying energies. Again, impressive results have been obtained for single-resonance Hamiltonians in terms of understanding the spectral features, semiclassical quantization and analysis of the energy splittings. However, multiresonant systems have not received much attention from this point of view. Sizable work has also been done from a different perspective, wherein one explores the signatures of resonances on the energy levels as a parameter in the Hamiltonian is varied.^{23–34} The importance of such works lies in the fact that states can be approximately assigned by following the energy diabats from a known limit to the actual physical Hamiltonian.^{59–61} In such energy correlation or equivalently level dynamics studies, the focus was predominantly on the nature of avoided crossings and their distributions. Earlier studies^{23–27} argued that the avoided crossing between pairs of energy levels implied that the corresponding states were involved in resonance. From this viewpoint, overlapping avoided crossings would be the analogue of overlapping resonances in the underlying classical system. Thus, it was conjectured^{23,25} that overlapping avoided crossings would lead to a criterion for quantum stochasticity in analogy to the Chirikov criterion⁶² for classical stochasticity threshold. Although the conjecture has some support for time-independent systems perturbed by a periodic time dependent potential,⁶³ later studies^{28–34} indicated that states involved in an isolated avoided crossing were not necessarily resonant. In the vicinity of an avoided crossing, the state mixing could as well be due to quantum tunneling. In fact, dynamical tunneling^{64,65} has been proposed⁶⁶ as a possible route to IVR in a certain class of molecules. Moreover, in case of multi-resonant systems, the two state avoided crossing scenario can get superseded by a three-state chaos-assisted tunneling^{67–70} process. Energy splittings due to chaos-assisted tunneling are fairly erratic^{67,70} and in particular can show algebraic dependence on \hbar rather than the usual exponential dependence. Hence, in absence of a clear relative measure of the competition between quantum and classical routes to state mixing, associating an isolated avoided crossing with the classical resonance is premature.

Given that avoided crossings do not unambiguously signal the presence of a resonance, one asks if there is any characteristic pattern in the level dynamics of a Hamiltonian that is indicative of a resonance. The primary goal of this paper is to answer the above question. There does exist an earlier work³³ wherein one such pattern was identified by investigating the behavior of the energy levels of a coupled oscillator system as the corresponding classical system went through a resonance. The pattern consisted of clusters of levels, each containing a number of curves that run roughly parallel to one another and a number of curves that undergo pairwise narrowly avoided

crossings. It was established that the parallel curves and narrowly avoided curves corresponded to resonant and nonresonant states, respectively. In this work, we take a different approach and identify characteristic patterns of the energy levels of a single-resonance Hamiltonian $H = H_0 + \tau V$ as the resonant strength τ is varied. It is now well-known^{71–73} that the evolution of the N energy levels with the coupling parameter can be mapped on to a Hamiltonian system with the energy levels corresponding to positions of N pseudoparticles and the coupling strength corresponding to a pseudotime variable. The resulting classical Hamiltonian describing the level and eigenstate dynamics of H has been shown⁷³ to be integrable since the equations of motion constitute a generalized Calogero–Moser^{74–76} system. Although we will not make an explicit use of the integrability structure, the prime focus will be on identifying the fingerprints of a classical resonance on the level velocities. This choice is motivated by two factors. The first one has to do with the numerical observation¹⁶ of energy diabats varying linearly at large values of the coupling constant. The second factor is related to the extensive work done⁷⁷ on uncovering universal and nonuniversal characteristics of nonintegrable Hamiltonians by systematic studies of the level velocities and their correlations.

We derive an expression for the level velocity associated with an eigenstate of a single-resonance Hamiltonian (section II). It is well-known that single-resonance Hamiltonians are classically integrable due to the existence of a conserved quantity called as the polyad number P . Consequently, all of the quantum eigenstates can be assigned. Analyzing the expression for the level velocities and noting the finiteness of the polyad number, one anticipates that the level velocities will, for some $\tau \geq \tau_c$, become constants. A rough estimate for the critical coupling constant τ_c is provided in section II.A. In general, more than one resonant state exists for a given value of the polyad, which is characterized by an excitation index. The level velocities of the group of states belonging to a specific polyad depend on the excitation index and give rise to a typical “fan” structure as τ is varied. On the basis of previous works¹⁶ showing the existence of isomorphic states occurring at definite polyad intervals, it is expected that the “fan” motif would repeat itself throughout the energy range. An analysis of the level velocities, as performed in section II.B, indicates that a simple relationship exists between the velocities of the isomorphic states at any given τ . As a consequence, the velocity of a given state can be approximately predicted from the velocity of the preceding isomorphic state. For $\tau \geq \tau_c$, the analysis in section II.B suggests that the asymptotic velocities for a general $m:n$ resonance scale with the polyad as $P^{(m+n)/2}$. In section III, we study a model two-mode 1:1 Hamiltonian and numerically confirm the predictions. In particular, it is shown that, for a 1:1 resonant state with excitation index ν , belonging to a polyad P , the asymptotic velocity is well approximated by $(P - 2\nu)$. Section IV concludes with a discussion on the possibility of using the present method for a dynamical assignment for the states of a multiresonant system.

II. Level Dynamics for Single-Resonance Hamiltonians

In this paper, we focus on a two-mode, single-resonance quantum Hamiltonian of the form

$$H_0(\mathbf{n}, \mathbf{a}, \mathbf{a}^\dagger) = H_0(\mathbf{n}) + \tau V(\mathbf{a}, \mathbf{a}^\dagger) \quad (1)$$

where H_0 is the zeroth order Hamiltonian

$$H_0(\mathbf{n}) = \sum_{k=1,2} \omega_k \left(n_k + \frac{1}{2} \right) + \sum_{k=1,2} \alpha_{kk} \left(n_k + \frac{1}{2} \right)^2 + \alpha_{12} \left(n_1 + \frac{1}{2} \right) \left(n_2 + \frac{1}{2} \right) \quad (2)$$

V is the resonant coupling term, and τ is the coupling strength. The operators \mathbf{n} , \mathbf{a} , and \mathbf{a}^\dagger are the number, annihilation, and creation operators for the two modes, respectively, which satisfy the standard harmonic oscillator relations $[a_k, a_l^\dagger] = \delta_{kl}$. For a $m:n$ resonance, the form of V is given by

$$V = (a_1)^\dagger (a_2)^n + (a_2) \mathbf{n} (a_1)^\dagger \quad (3)$$

It is well-known that the above single-resonance Hamiltonian has a conserved quantity known as the polyad number.^{53,54} This is due to the fact that the polyad operator $P = (n/m)n_1 + n_2$ commutes with the Hamiltonian H . As a result, the Hamiltonian is block diagonal with the blocks characterized by the eigenvalues of P .

In the rest of this paper, we will denote the eigenstates and the associated eigenvalues of the Hamiltonian H by $|\alpha(\tau)\rangle$ and $x_\alpha(\tau)$, respectively, with $H(\tau)|\alpha(\tau)\rangle = x_\alpha(\tau)|\alpha(\tau)\rangle$. The objective of this work is to study the level dynamics, i.e., the evolution of the eigenvalues $x_\alpha(\tau)$ with resonance coupling strength τ in order to identify the signatures of the underlying classical resonance. The eigenstates and eigenvalues for a given τ are obtained by numerically solving the Schrödinger equation in the zeroth order number basis $|\mathbf{n}\rangle$. Thus, one can express the eigenstate in terms of the zeroth order number basis as $|\alpha(\tau)\rangle = \sum_{\mathbf{n}} c_{\mathbf{n}\alpha}(\tau) |\mathbf{n}\rangle$. Eigenstates of a single-resonance Hamiltonian have to respect the polyad constraint, and hence, we can be more precise and write $|\alpha(\tau)\rangle = \sum_{\mathbf{n} \in P} c_{\mathbf{n}\alpha}(\tau) |\mathbf{n}\rangle$.

In the study of the level dynamics of $H(\tau)$, an important quantity is the level velocity $\dot{x}_\alpha(\tau) \equiv dx_\alpha/d\tau$ associated with the state $|\alpha(\tau)\rangle$. The level velocity for a given state, as obtained using the Hellmann–Feynman theorem, is

$$\dot{x}_\alpha(\tau) = \langle \alpha(\tau) | V | \alpha(\tau) \rangle \quad (4)$$

Inserting complete sets of states into eq 4 the expression for the level velocity can be written as

$$\begin{aligned} \dot{x}_\alpha(\tau) &= \sum_{\mathbf{n} \in P} \sum_{\mathbf{n}' \in P'} \langle \alpha(\tau) | \mathbf{n} \rangle \langle \mathbf{n} | V | \mathbf{n}' \rangle \langle \mathbf{n}' | \alpha(\tau) \rangle \\ &= \sum_{\mathbf{n} \in P} \sum_{\mathbf{n}' \in P'} c_{\mathbf{n}\alpha}^*(\tau) c_{\mathbf{n}'\alpha}(\tau) V_{\mathbf{n}\mathbf{n}'} \end{aligned} \quad (5)$$

where we have denoted the matrix element $\langle \mathbf{n} | V | \mathbf{n}' \rangle$ by $V_{\mathbf{n}\mathbf{n}'}$. Due to the polyad constraint, it is clear that the product $c_{\mathbf{n}\alpha}^* c_{\mathbf{n}'\alpha}$ vanishes unless $P = P'$. In addition, as $V_{\mathbf{n}\mathbf{n}'}$ also vanishes if $\mathbf{n} = \mathbf{n}'$, one obtains

$$\dot{x}_\alpha(\tau) = \sum_{\substack{\mathbf{n}, \mathbf{n}' \in P \\ \mathbf{n} \neq \mathbf{n}'}} c_{\mathbf{n}\alpha}^*(\tau) c_{\mathbf{n}'\alpha}(\tau) V_{\mathbf{n}\mathbf{n}'} \quad (6)$$

as the level velocity associated with an eigenstate $|\alpha(\tau)\rangle$. Note that the presence of the matrix element $V_{\mathbf{n}\mathbf{n}'}$ gives a strong local character to the level velocity since $V_{\mathbf{n}\mathbf{n}'} = 0$ if \mathbf{n} and \mathbf{n}' are not connected by the resonance. It is clear from the above expression that if the state $|\alpha(\tau)\rangle$ is nonresonant, then $\dot{x}_\alpha(\tau) = 0$ and hence, as expected, there is no change in the energy of the state as the coupling strength is varied. In what follows, we will take all the coefficients to be real without any loss of generality.

A few important observations can be made about the level dynamics of H by understanding the low and high τ limits of eq 6. First, note that the entire τ dependence is in the basis coefficients. For small values of τ , most of the states will be nonresonant, and $\dot{x}_\alpha(\tau) \approx 0$. As the value of τ is increased, the coefficients $c_{\mathbf{n}\alpha}(\tau)$ also change, making the level velocities finite for states that come under the influence of the resonance. However, a finite value of the polyad associated with a resonant state implies that the number of zeroth order states that participate and contribute to the resonant eigenstate is finite. This leads one to expect that beyond a certain critical coupling strength τ_c , the level velocity should become relatively insensitive to changes in τ . Thus, in the limit of large τ the level velocities are constants, i.e., $\dot{x}_\alpha(\tau) \approx v_\alpha$, with v_α being independent of τ . An estimate for v_α would require one to know the asymptotic value of the basis coefficients $c_{\mathbf{n}\alpha}(\tau)$ for large τ . A tempting choice is to set $c_{\mathbf{n}\alpha}(\tau) \approx N_P^{-1/2}$ for all \mathbf{n} , with N_P denoting the number of zeroth order states in a given polyad P . However, such a choice is erroneous since a single-resonance Hamiltonian is classically integrable due to the existence of the polyad. Hence, one expects a regular spectrum associated with the quantum Hamiltonian. On the other hand, only in the extreme statistical limit does one anticipate⁷⁸ $c_{\mathbf{n}\alpha}(\tau) \approx N_P^{-1/2}$. Thus, for an integrable system, in general, such an approximation is invalid. Nevertheless, it is reasonable to assume that the coefficients and hence the product of coefficients in the expression for $\dot{x}_\alpha(\tau)$ attain a limiting value around τ_c leading to constant level velocities for $\tau \geq \tau_c$. One way of finding the asymptotic value of the coefficients is to investigate the large τ asymptotics for the corresponding Schrödinger equation which is known,⁷⁹ in a certain limit, to be the Mathieu equation. Such an approach would also yield the critical coupling constant τ_c , which is of significant interest for understanding the level dynamics of the system. In this work, we do not perform such an analysis and provide a rough estimate for τ_c , with the focus being more on a phenomenological description of the level dynamics. Analyzing the expression for $\dot{x}_\alpha(\tau)$ for specific classes of resonant states, as shown below, one predicts that fairly simple expressions should exist for v_α .

A. Estimate for τ_c Based on the Chirikov Approximation.

As pointed out in the previous section, the constancy of the level velocity for $\tau \geq \tau_c$ is due to the finiteness of P . Intuitively, one anticipates that if the classical resonance width $w(\tau)$ for $\tau = \tau_c$ is on the order of the number of zeroth order quantum states for a given P , then the coefficients $c_{\mathbf{n}\alpha}(\tau)$ of the state $|\alpha(\tau)\rangle$ would not change much with increasing τ . This suggests that τ_c can be estimated by setting $w(\tau_c) \simeq N_P$, with $w(\tau)$ obtained by a Chirikov analysis⁶² of the classical resonance Hamiltonian.

To obtain $w(\tau)$, we construct the classical limit Hamiltonian for the two-mode quantum Hamiltonian $H(\tau)$ by using the standard correspondence⁸⁰

$$\mathbf{a} \leftrightarrow \mathbf{I}^{1/2} e^{-i\theta} \quad \mathbf{a}^\dagger \leftrightarrow \mathbf{I}^{1/2} e^{i\theta} \quad (7)$$

where (\mathbf{I}, θ) are the classical action–angle variables. The resulting classical limit $m:n$ resonant Hamiltonian is

$$H = \sum_{k=1,2} (\omega_k I_k + \alpha_{kk} I_k^2) + \alpha_{12} I_1 I_2 + 2\tau \sqrt{I_1^m I_2^n} \cos(m\theta_1 - n\theta_2) \quad (8)$$

The two-dimensional Hamiltonian above can be transformed to a one-dimensional Hamiltonian by using the generating

function⁸¹

$$F_2(I, J_\rho, \phi, \rho) = \frac{1}{2} J_\rho (m\theta_1 - n\theta_2) + I\theta_2 \quad (9)$$

which generates a canonical transformation $(\mathbf{I}, \theta) \rightarrow (I, J_\rho, \phi, \rho)$. The resulting one-dimensional classical limit Hamiltonian is

$$H = \frac{\gamma}{4} J_\rho^2 - \frac{1}{2} (\Omega + QI) J_\rho + C + 2\bar{\tau} J_\rho^{m/2} \left(\frac{2I}{n} - J_\rho \right)^{n/2} \cos 2\rho \quad (10)$$

with $C = \omega_2 I + \alpha_{22} I^2$, $\Omega = n\omega_2 - m\omega_1$, $Q = 2n\alpha_{22} - m\alpha_{12}$, $\gamma = m^2\alpha_{11} + n^2\alpha_{22} - mn\alpha_{12}$, and $\bar{\tau} = (m^m n^n 2^{-(m+n)})^{1/2} \tau$. It is clear that the action $I = (n/m)I_1 + I_2$ is a constant of the motion. Thus, the classical limit Hamiltonian is integrable, and I is the classical analogue of the polyad number P .

To estimate the resonance width, we expanded the one-dimensional classical Hamiltonian about the resonant value of $J_\rho = J_\rho^r = \gamma^{-1}(\Omega + QI)$ to obtain the resonant Hamiltonian

$$H_r(I, \delta J_\rho, \rho) \equiv H(I, J_\rho^r + \delta J_\rho, \rho) - H_0(I, J_\rho^r) \approx \frac{1}{4} \gamma (\delta J_\rho)^2 + 2\bar{\tau} (J_\rho^r)^{m/2} \left(\frac{2I}{n} - J_\rho^r \right)^{n/2} \cos 2\rho \quad (11)$$

The Hamiltonian H_r is recognized to be the standard one-dimensional pendulum Hamiltonian,^{62,81} and thus, the width is given by

$$w(\tau) = \left(\frac{16\bar{\tau}}{\gamma} \right)^{1/2} (J_\rho^r)^{m/4} \left(\frac{2I}{n} - J_\rho^r \right)^{n/4} \quad (12)$$

At this stage, we set $w(\tau_c) \approx N_P$ to obtain an estimate for the critical coupling constant as

$$\tau_c \approx r_{mn} \gamma N_P^2 (m J_\rho^r)^{-m/2} (2I - n J_\rho^r)^{-n/2} \quad (13)$$

with $r_{mn} = (2^{8-(m+n)})^{-1/2}$. For single-resonance systems, N_P scales linearly with P , and hence, the critical coupling scales as P and \sqrt{P} for the 1:1 and 1:2 resonant systems, respectively. On the classical side, it is expected that the Poincaré surface of section should be filled up with resonant tori for $\tau \sim \tau_c$.

B. Level Velocities for Isomorphic States. The states of a single-resonance Hamiltonian can be completely assigned because of the existence of the polyad number P . For a given value of P , there can be many resonant states, and the total number of states is related to the classical width $w(\tau)$ of the resonance zone. The manifold of resonant states for fixed P can be characterized by an excitation quantum number $\nu = 0, 1, \dots$, related to the number of nodes for the state. Thus, a general resonant state will be denoted by $|P; \nu\rangle$, with an associated level velocity $\dot{x}_\alpha^{(\nu)}(\tau; P)$.

Recent work^{16,82} has shown that the slope of the classical resonance center line, as viewed in the quantum discrete \mathbf{n} space, is an important parameter for understanding the resonant states. In particular, as is well-known, quantum states organize themselves around the classical resonance line. However, a more detailed observation is that isomorphic resonant states appear with a periodicity identical to that of the slope of the classical resonance line. These states are isomorphic in the sense that they have very similar amplitude distributions in the zeroth order basis. Moreover, a study of the Husimi distribution functions of the isomorphic states indicated¹⁶ that they “live” in identical, resonant, regions of the phase space. It is thus possible to organize the entire set of states in terms of such isomorphic

families. An analysis of the single-resonance Schrödinger equation, in terms of Floquet solutions of the resulting Mathieu equation, reveals⁸² that such isomorphic states appear with a polyad spacing $\Delta P = (m\rho + n)$ for a general $m:n$ case. The classical-quantum correspondence is highlighted by the appearance of the slope

$$\rho \equiv \frac{n\alpha_{12} - 2m\alpha_{11}}{m\alpha_{12} - 2n\alpha_{22}} \quad (14)$$

of the classical resonance line in the expression for ΔP . Clearly, the slope ρ itself is a function of the anharmonicity parameters involved in the zeroth order Hamiltonian H_0 .

The above discussion suggests that the level velocities for isomorphic states should be related in a simple fashion. Consider two isomorphic states which belong to the polyads P and $P + \Delta P$. The basis coefficients of these states are nonzero for $\mathbf{n} \in P$ and $\bar{\mathbf{n}} \in P + \Delta P$, respectively. Since the states are isomorphic, one expects

$$c_{\mathbf{n}\alpha}^{(\nu)}(\tau) c_{\bar{\mathbf{n}}\alpha}^{(\nu)}(\tau) \approx c_{\bar{\mathbf{n}}\alpha}^{(\nu)}(\tau) c_{\mathbf{n}\alpha}^{(\nu)}(\tau) \quad (15)$$

In the above equation, $\bar{\mathbf{n}} = \mathbf{n} + \mathbf{d}_\rho$ with a similar expression for $\bar{\mathbf{n}}'$ and $\mathbf{d}_\rho = (m, m\rho)$. In other words, a state at polyad P is displaced along the classical resonance line to a isomorphic state at polyad $P + \Delta P$. In general, the approximation eq 15 is valid for moderate values of the coupling strength τ . This is due to the fact that the existence of isomorphic states requires the resonance width to vary slowly over the entire action space. Typically, the resonance width increases as one goes to higher energies (hence actions), and thus, the resonance strength felt by states at $P + \Delta P$ can be substantially larger. This leads to a breakdown of the approximation since the basis coefficients at \mathbf{n} as compared to those at $\mathbf{n} + \mathbf{d}_\rho$ are quite different. It is possible to come up with corrections to eq 15, but we will not pursue such schemes in this work. However, it is important to note that for states that exhibit localization at any P , the approximation is a valid one, and the level velocities, as shown below, can indicate the existence of families of localized isomorphic states.

Within the approximation eq 15, one immediately obtains the level velocity of the isomorphic state $|P + \Delta P; \nu\rangle$ as

$$\begin{aligned} \dot{x}_\alpha^{(\nu)}(\tau; P + \Delta P) &= \sum_{\bar{\mathbf{n}} \neq \bar{\mathbf{n}}'}^{\bar{\mathbf{n}}, \bar{\mathbf{n}}' \in P + \Delta P} c_{\bar{\mathbf{n}}\alpha}^{(\nu)}(\tau) c_{\bar{\mathbf{n}}'\alpha}^{(\nu)}(\tau) V_{\bar{\mathbf{n}}\bar{\mathbf{n}}'} \\ &\approx \sum_{\mathbf{n} \neq \mathbf{n}'}^{\mathbf{n}, \mathbf{n}' \in P} c_{\mathbf{n}\alpha}^{(\nu)}(\tau) c_{\mathbf{n}'\alpha}^{(\nu)}(\tau) V_{\mathbf{n} + \mathbf{d}_\rho, \mathbf{n}' + \mathbf{d}_\rho} \end{aligned} \quad (16)$$

To relate the level velocities of two isomorphic states, consider the difference in the velocities

$$\begin{aligned} \delta \dot{x}_\alpha^{(\nu)}(\tau) &= \dot{x}_\alpha^{(\nu)}(\tau; P + \Delta P) - \dot{x}_\alpha^{(\nu)}(\tau; P) \\ &\approx \sum_{\mathbf{n}, \mathbf{n}'}^{\mathbf{n}, \mathbf{n}' \in P} c_{\mathbf{n}\alpha}^{(\nu)}(\tau) c_{\mathbf{n}'\alpha}^{(\nu)}(\tau) [V_{\mathbf{n} + \mathbf{d}_\rho, \mathbf{n}' + \mathbf{d}_\rho} - V_{\mathbf{n}, \mathbf{n}'}] \end{aligned} \quad (17)$$

The matrix element $V_{\mathbf{n}\mathbf{n}'}$ for a general $m:n$ resonance has the standard form

$$V_{\mathbf{n}\mathbf{n}'} = \sqrt{V(n_1, n_2)} \delta_{n'_1, n_1 - m} \delta_{n'_2, n_2 + n} + \sqrt{\bar{V}(n_1, n_2)} \delta_{n'_1, n_1 + m} \delta_{n'_2, n_2 - n} \quad (18)$$

where $V(n_1, n_2)$ and $\bar{V}(n_1, n_2)$ are polynomials of order m and n

in n_1 and n_2 , respectively. The form of $V_{nn'}$ suggests that the second-order variation in $V_{nn'}$ with \mathbf{n} is fairly small, i.e., $\Delta^2 V \sim O(1/n)$. Thus, the quantity $(V_{\mathbf{n}+\mathbf{d},\mathbf{n}'+\mathbf{d}_\rho} - V_{\mathbf{n},\mathbf{n}'})$ is essentially constant over a range of \mathbf{n} and depends primarily on \mathbf{d}_ρ and P . This implies that one can write

$$\delta \dot{x}_\alpha^{(\nu)}(\tau) \approx 2c_\alpha^{(\nu)}(\tau)f(\rho, P) \quad (19)$$

where the form of the function f is specific to the resonance and

$$c_\alpha^{(\nu)}(\tau) \equiv \sum_{n_1, n_2 \in P} c_{n_1, n_2; \alpha}^{(\nu)}(\tau) c_{n_1 - m, n_2 + n; \alpha}^{(\nu)}(\tau) \quad (20)$$

Hence, given the level velocity of the state $|P; \nu\rangle$, the above relation shows that one can approximately predict the level velocity of the isomorphic state $|P + \Delta P; \nu\rangle$ with $\Delta P = (m \rho + n)$ for a given τ . However, at this level of approximation, the value of the predicted level velocity is accurate for localized states. In particular, here one expects the predicted velocities to be accurate for the $\nu = 0$ states only. The specific form of the function f can be worked out for the various resonances, and for a 1:1 resonance, it is easy to show that to leading order

$$f(\rho, P) \approx \frac{1}{2}(1 + \rho) = \frac{1}{2}\Delta P \quad (21)$$

Thus, for the isomorphic states with $\nu = 0$ corresponding to a 1:1 resonance, we have the result that $\delta \dot{x}_\alpha^{(0)}(\tau) \approx c_\alpha^{(0)}(\tau)\Delta P$.

Note that the above analysis is incomplete in the sense that the ν dependence of the level velocities is not obtained. As discussed earlier, the determination of $c_\alpha^{(\nu)}(\tau)$ in the large coupling limit is nontrivial. However, the eq 20 can be interpreted⁸³ as the overlap between the state and another fictitious state at the same value of P , obtained by shifting the actual state. This suggests, at least for $\tau \sim \tau_c$, that the state with $\nu = 0$ has the maximum velocity. This interpretation in terms of overlaps suggests that $c_\alpha^{(0)}(\tau) \approx 1$ for $\tau \geq \tau_c$. Increasing ν will lead to smaller overlap due to the sign mismatches, and hence, the velocity decreases with increasing ν . Thus, for a given set of states in a polyad P , the asymptotic velocities decrease with increasing ν , and this gives rise to a diabatic fan-like structure in the energy correlation diagram. For now, in the large coupling limit, we can combine the result $c_\alpha^{(0)} \approx 1$ with $\delta \dot{x}_\alpha^{(0)} \approx c_\alpha^{(0)}\Delta P$ to obtain the asymptotic level velocity of the 1:1 resonant state $|P; 0\rangle$ as

$$v_\alpha \equiv \dot{x}_\alpha^{(0)} \approx P \quad (22)$$

As discussed above, v_α for states with nonzero ν will decrease with increasing ν . In the next section, computational studies suggest that in the large coupling limit the asymptotic velocity of a 1:1 state $|P; \nu\rangle$ is approximated rather well by $v_\alpha \approx (P - 2\nu)$. Analysis along similar lines for a general $m:n$ resonance system indicates that in the large coupling limit the asymptotic velocity of a state $|P; 0\rangle$ obeys the rule

$$v_\alpha \propto P^{(m+n)/2} \quad (23)$$

III. Example of a Model 1:1 System

In this section, we compute level velocities for a model 1:1 resonant Hamiltonian with $\omega_1 = 1$, $\omega_2 = 0.8$, $\alpha_{11} = -0.04$, $\alpha_{12} = 0$, and $\alpha_{22} = -0.02$. With these parameter values, the slope of the classical resonance line is $\rho = +2$. Thus isomorphic states are expected with a polyad spacing $\Delta P = 3$.

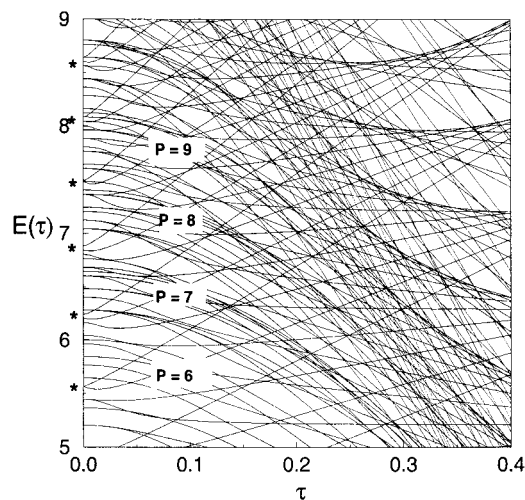


Figure 1. Level dynamics for the 1:1 resonance system. The fans associated with each polyad are indicated by *. The respective polyad values are also shown in the figure. The number of states in each fan increases since the resonance width increases with increasing energy.

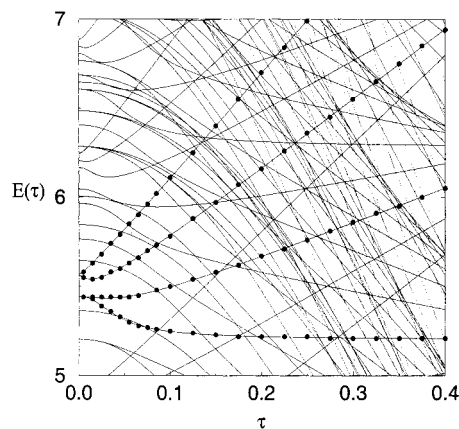


Figure 2. Level dynamics for the integrable 1:1 case. The fan formed by the states belonging to the polyad $P = 6$ is shown. The solid points correspond to resonant states as identified in the (I_1, I_2) space.

In Figure 1, we show the variation of the energies with the resonance strength τ . Two important features can be identified from Figure 1. First, the cluster of states associated with a polyad P is seen to form a fan-like structure. The states in this fan are undergoing large variations with the coupling strength τ . Similar-looking fans appear with a periodicity of 2, which is a consequence of the slope of the classical resonance line. It is expected that isomorphic states will show isomorphic level dynamics. The second observation, evident from Figure 1, is that for large τ the level velocities are becoming constants. In fact, for large values of τ , one sees streaks of straight lines—some with negative slopes and others with positive slopes. As discussed in the previous section, the negative slopes, i.e., negative asymptotic level velocities are associated with large ν states.

We now focus on one of the fans to show its structure and understand the ν dependence of the asymptotic level velocities v_α . In Figure 2, the fan associated with the states belonging to the polyad $P = 6$ is shown. Four states corresponding to $\nu = 0, 1, 2, 3$ are highlighted in the figure. The states at various values of τ were identified in the (n_1, n_2) state space. The classical resonance center line and widths in the action space (I_1, I_2) served as a template to identify the nature of the quantum states. Among the four states shown, the state $|6; 0\rangle$ has the largest variation, and the state $|6; 3\rangle$ has the smallest variation with τ . For this

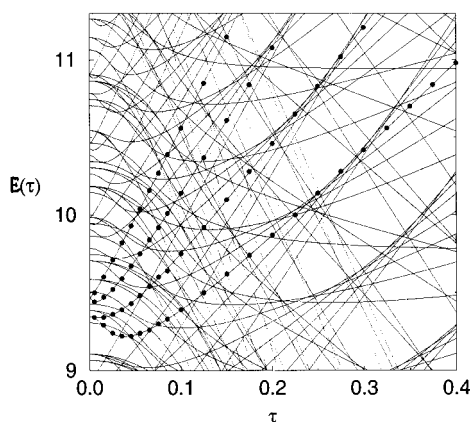


Figure 3. Same as in Figure 2 for states belonging to $P = 12$. This fan is isomorphic to the one at $P = 6$ shown in Figure 2.

value of the polyad, the critical coupling constant is estimated to be $\tau_c \approx 5.3 \times 10^{-2}$. It is clear from Figure 2 that the level velocities corresponding to the states $\nu = 0$ and 1 are approximately constant beyond the estimated τ_c . However, note that as far as the states $\nu = 2$ and 3 are concerned, the estimate for τ_c is not very accurate. The reason for this underestimation of τ_c has to do with the fact that our analysis was based entirely on a Chirikov criteria and hence essentially classical. The Chirikov estimate is thus insensitive to ν and only depends on P . A better estimate would necessarily have to be quantum or semiclassical in nature which would account for the ν dependence of a quantum state. An important observation concerning the state $|6;3\rangle$ is that the asymptotic level velocity $v_\alpha \approx 0$. However, this state is resonant, and the vanishing level velocity is due to the particular form of v_α for a 1:1 resonance as discussed below. The particular set of parameters chosen in this section imply that isomorphic quantum states should appear with a polyad spacing of three. Thus, one anticipates that the specific behaviour of the states with varying τ observed for $P = 6$ should manifest at polyad values $P = 9$ and 12 and so on. In Figure 3, we show one such isomorphic fan at $P = 12$ highlighting the four states, isomorphic to those at $P = 6$, as in Figure 2. For this value of the polyad, the critical coupling is estimated to be about 9.8×10^{-2} . Notice the similar variations of the states $|6;\nu\rangle$ and $|12;\nu\rangle$ with τ . It is interesting to note that the $\nu = 0$ state and, to some extent, the $\nu = 1$ state do respect the estimated τ_c irrespective of the polyad to which they belong.

Since the states belonging to polyads $P = 6, 9$, and 12 are isomorphic, we can test the approximation (eq 16) in this case. According to eq 16 the velocity of a state $|P + \Delta P; \nu\rangle$ can be approximately obtained by rigidly translating the corresponding isomorphic state $|P; \nu\rangle$ along the classical resonance line. In Figure 4, we compare the velocities computed with the approximation to the actual numerical values for a coupling strength of $\tau = 5 \times 10^{-2}$. It is seen that the approximation is very good for the $\nu = 0$ state and progressively becomes worse as ν increases. Incidentally, this indicates that the $\nu = 0$ state is much more localized in the resonance channel as compared to the higher ν states. The reasons for this behavior has been discussed earlier and has to do with the fact that the coupling strength seen by a state at $P + \Delta P$ is larger than that seen by a state at P . Thus, one computes the velocities for states $|P + \Delta P; \nu\rangle$ at an effective coupling strength $\tau' < \tau$ within the approximation eq. (16). For the current example of 1:1 parameters, it is easy to show that $(\tau' - \tau)/\tau \approx \Delta P/P$. Correcting for the effective coupling strength leads to very good agreement for all the states.

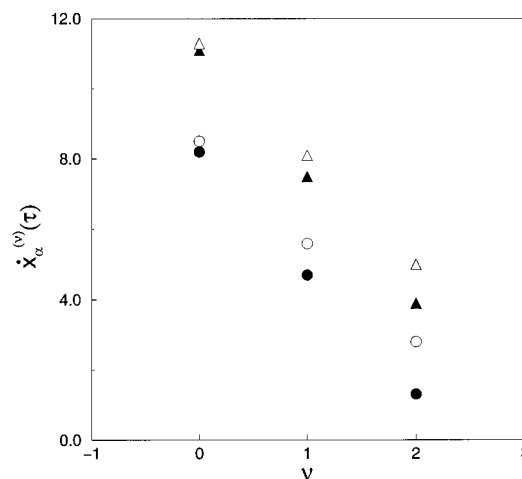


Figure 4. Velocities of isomorphic states according to the approximation eq 16, indicated by filled symbols. The value of the coupling strength is 5×10^{-2} . The circles and triangles correspond to $P = 6$ and to $P = 12$, respectively. Numerically exact values are shown as open symbols.

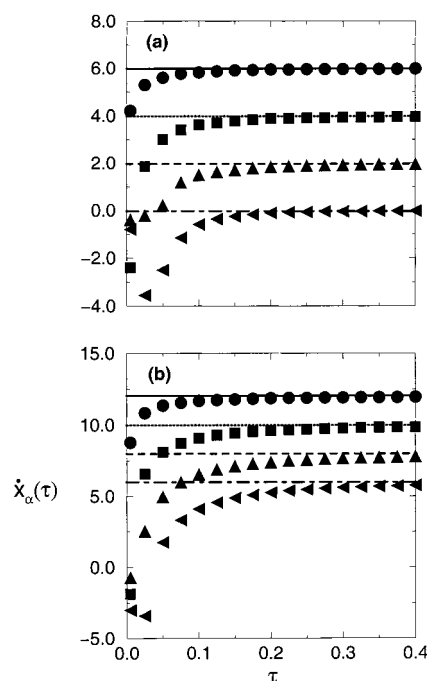


Figure 5. Variation of the level velocities with τ . (a) Results for $P = 6$ are shown for the various states $|P; \nu\rangle$ with $\nu = 0$ (circles), $\nu = 1$ (squares), $\nu = 2$ (up triangles), and $\nu = 3$ (left triangles). (b) Same as in panel a but for $P = 12$. In both the figures, the asymptotic limit result $(P - 2\nu)$ are shown as straight lines.

In Figure 5, the variations in the velocities x_α with τ for the states belonging to $P = 6$ and 12 are shown. The velocities are becoming constants for $\tau \geq \tau_c$, and in accordance with the conclusion from the last section, the $\nu = 0$ states indeed have asymptotic velocities $v_\alpha \approx P$. More importantly, the asymptotic velocities v_α for states in a given polyad are seen to differ by approximately a factor of 2. This suggests that the ν dependence of v_α is quite simple and given by

$$v_\alpha(P; \nu) = P - 2\nu \quad (24)$$

Computation of the level velocities for many different values of the parameters, i.e., different Hamiltonians, establishes the result 24 to be fairly accurate. The comparison for four different

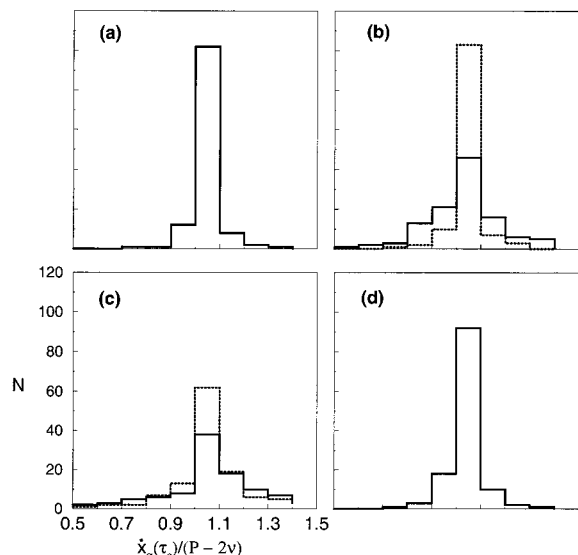


Figure 6. Comparison of the asymptotic velocity estimate $(P - 2\nu)$ with the computed values $\tilde{x}_\alpha(\tau_c)$ for different H_0 parameters. In all the figures, $\tau_c = 4 \times 10^{-1}$. In panels b and d, the dotted histogram shows the result for $\tau_c = 6 \times 10^{-1}$.

1:1 Hamiltonians is shown in Figure 6, where we plot the ratio $\tilde{x}_\alpha^{(\nu)}(\tau_c)/(P - 2\nu)$ for states with polyad values $P \leq 15$. The accuracy of the expression for the asymptotic velocity is evident from the figure. The spread as seen in Figure 6 results from the dependence of τ_c on ν . Thus, for a 1:1 resonance, $\delta\tilde{x}_\alpha^{(\nu)} \approx \Delta P$. An interesting consequence of the above result is that certain resonant states could exhibit zero level velocity for $\tau \geq \tau_c$. For instance, the state $|6;3\rangle$ in Figure 2 shows zero level velocity despite being a resonant state. It is clear that a naive interpretation of the correlation diagram might mislead one to label the state as nonresonant.

In almost all of the studies on level dynamics,^{84–91} the key quantities of interest are the variance of the level velocities and the curvature, i.e., \tilde{x}_α distribution. The variance of the level velocities is defined as

$$\sigma^2(\tau, N) = \frac{1}{N} \sum_{\alpha} (\tilde{x}_\alpha^{(\nu)}(\tau))^2 - \left(\frac{1}{N} \sum_{\alpha} \tilde{x}_\alpha^{(\nu)}(\tau) \right)^2 \quad (25)$$

An understanding of σ^2 is crucial to uncovering possible universalities in parametric level correlations. Most of the efforts toward this end have concentrated on strongly chaotic systems. A recent work⁹¹ has discussed the case of systems with mixed phase space. It was observed that the transition to classical chaos is accompanied by a corresponding transition of σ^2 from a quadratic to linear N dependence. Having obtained the asymptotic level velocities for an integrable 1:1 resonant system we are in a position to evaluate the variance $\sigma^2(\tau_c, N_P)$ for the cluster of states belonging to a polyad P . The evaluation is straightforward since

$$\begin{aligned} \sigma^2(\tau_c, N_P) &= \frac{1}{N_P} \sum_{\nu=0}^{\nu_{\max}} (P - 2\nu)^2 - \left[\frac{1}{N_P} \sum_{\nu=0}^{\nu_{\max}} (P - 2\nu) \right]^2 \\ &= \frac{1}{3} (N_P^2 - 1) \end{aligned} \quad (26)$$

and $N_P = \nu_{\max} + 1$. Thus, $\sigma^2(\tau_c, N_P) \sim N_P^2$, which is in agreement with the recent work.⁹¹

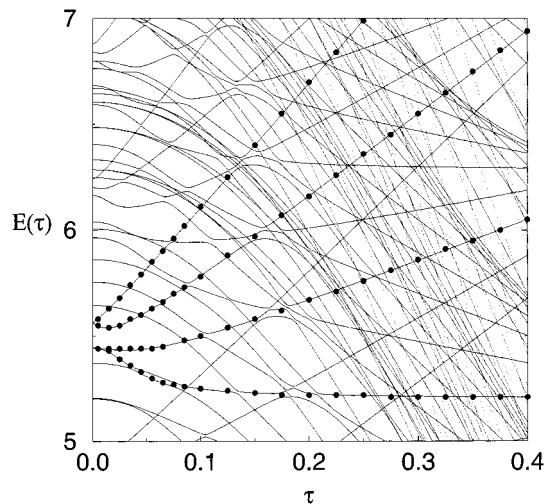


Figure 7. Level dynamics in the nonintegrable case. The variation with the 1:1 resonance strength is shown with the 1:2 coupling strength fixed at 5×10^{-3} . The integrable 1:1 fan (solid points) corresponding to $P = 6$ (cf. Figure 2) is superimposed for comparison.

IV. Discussion and Summary

The results of the previous sections clearly show that the fingerprint of a classical resonance in the quantum eigenlevel dynamics are the diabatic fan structures. Each fan corresponds to the various states $|P; \nu\rangle$ in a polyad P . One can imagine assigning the quantum states belonging to a particular polyad by computing the asymptotic level velocities. This, of course, is an unnecessary exercise for a single-resonance Hamiltonian but a useful point of view for multiresonant Hamiltonians. Multiresonant Hamiltonians are classically nonintegrable, and hence, chaos can play a significant role in the attempts to assign the high energy states.

An important issue that arises, in the context of the present work, is the possibility of assigning the states of a multiresonant system. More specifically, one asks if it is possible to use the integrable limit fans as a template to identify the dominant resonance contributing to the structure of an eigenstate. In order for such a scheme to work, one needs measures for gauging the extent to which a given state is scarred by the various underlying resonances. As a first step, with such a goal in mind, we show the effect of adding a weak 1:2 resonance on the eigenlevel dynamics considered in the previous section. In Figures 7 and 8, we show the counterparts of Figures 2 and 3, respectively, with a weak (coupling strength of 5×10^{-3}) 1:2 resonance present in addition to the 1:1 resonance. The integrable limit fans have been shown as points on the same figure. Note that most of the crossings in the integrable limit have become avoided crossings in this nonintegrable situation.

For the case of integrable limit $P = 6$ (cf. Figure 7), we see that the 1:2 has had no major effect and the states are essentially scarred by the 1:1 resonance. In this case, the integrable limit fan structure is robust through the avoided crossings. This agrees well with the fact that the location of the 1:2 resonance in the (I_1, I_2) space is such that there is a very weak influence on the states belonging to the $P = 6$ manifold. The number of avoided crossings increases as one goes up in energy as shown in Figure 8 corresponding to the integrable limit $P = 12$ case. However, for the low ν cases, one observes that the integrable fan structure is fairly robust. This suggests that the 1:1 resonance is dominating the structure of the eigenstates in this energy regime. For very large values of the 1:1 coupling parameter one sees, as expected, a similar behavior as in the integrable situation.

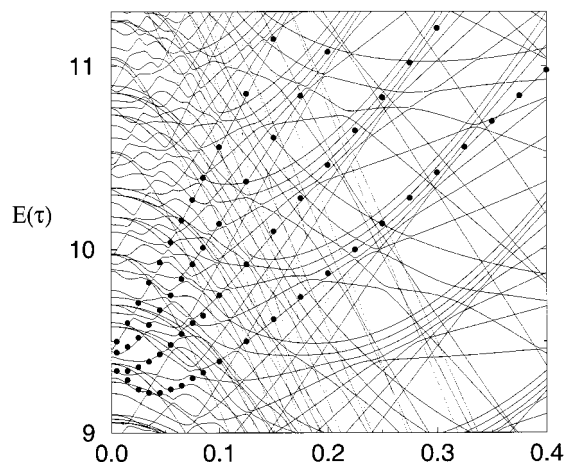


Figure 8. Same as in Figure 7 but for the higher-energy regimes. The integrable limit $P = 12$ fan (cf. Figure 3) is superimposed for comparison.

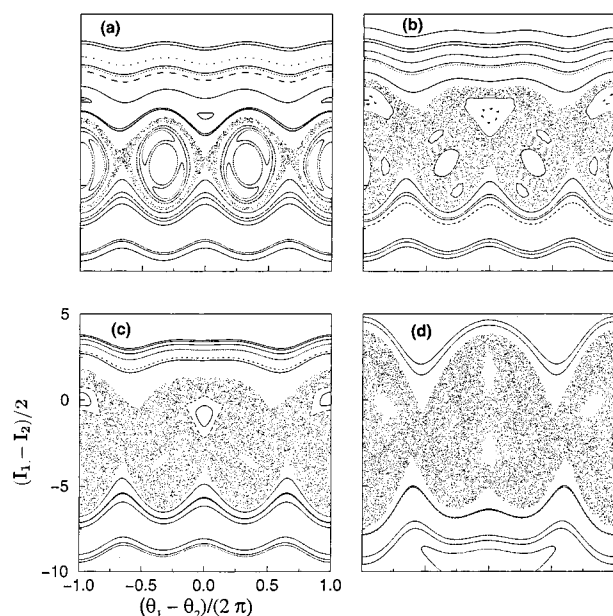


Figure 9. Poincaré surface of sections at different 1:1 coupling strengths with the 1:2 resonance strength fixed at 5×10^{-3} . Energy corresponds approximately to the $P = 12$ region. (a) $\tau = 1 \times 10^{-3}$ (b) $\tau = 5 \times 10^{-3}$ (c) $\tau = 10 \times 10^{-3}$, and (d) $\tau = 50 \times 10^{-3}$.

The important point, however, is that the linear variation with coupling can be clearly seen even in the nonintegrable situation.

The nature of the classical dynamics is illustrated in Figure 9 as a Poincaré surface of section at energies approximately corresponding to the $P = 12$ case. Note that the linear variation of the energy levels persists despite the presence of extensive stochasticity in the phase space. This indicates that the states are getting scarred by the resonance. A similar observation has been made^{84,87} in the context of level dynamics of the stadium billiard system. In the stadium billiard, the presence of the bouncing ball periodic orbits leads to parametric level motion running as straight lines. These linearly varying level curves were identified⁸⁴ as soliton-like structures and have been linked to the existence of extensive scarring of the eigenstates by the classical periodic orbits. This is in turn reflected in the curvature distribution as an excess contribution, over the universal prediction, around the small curvature regions.⁸⁷

It is now known that the small curvature distribution is nonuniversal, i.e., system-specific. In fact, one now anticipates that the solitonic structures will arise in a level dynamics

whenever there is extensive scarring present in the system. For example, another system where such behavior has been observed is the hydrogen atom in a strong uniform magnetic field.⁸⁷

The results presented in this paper suggest that such solitonic structures are indeed the fingerprints of an underlying classical resonance. In this sense, every distinct resonance has its own solitonic signature, in the form of “solitonic fans”, in the level dynamics. In earlier works,^{84,87} the solitonic features have been associated with scarring of the eigenstate by periodic orbits. However, it is fair to expect that scarring in systems with mixed phase space can also be due to higher dimensional tori. Such a viewpoint has to be adopted especially in systems where periodic orbits alone are not sufficient to understand the phase space structure of the system. For example, in a recent work¹⁶ on the assignment of highly excited states of H_2O , evidence of scarring by resonant 2-tori is observed in the level dynamics. The nonuniversal nature associated with the solitonic structures indicates the possibility of extracting system specific information in the multiresonant situations. In particular, one hopes for a measure which will identify the dominant resonances contributing to the structure of an eigenstate. Recent works^{92,93} have suggested a measure involving the overlap intensity-level velocity correlation coefficient which is suitable for exploring the phase space localization features of eigenstates. Another suggestion⁸⁷ based on the curvature distribution falls short of our expectations since information is provided in an overall sense and not at an individual eigenstate level. A knowledge of the dominant resonances giving rise to the features of a particular eigenstate provides information about the expected dynamical behavior of the system. A key advantage of such an approach is that the study of three or more degrees of freedom systems can be undertaken without recourse to the usual route, difficult if not impossible at the moment, involving the computation, visualization, and correlation of the Poincaré surface of section and the Husimi distribution functions. Work is in progress in our group to determine the appropriate measures of scarring and the assignment of highly excited states of multimode, multiresonant systems from the viewpoints advanced in this paper.

Acknowledgment. This work is supported by grants from the Department of Science and Technology and the Council of Scientific and Industrial Research.

References and Notes

- (1) Ezra, G. S. *Adv. Classical Trajectory Methods* **1998**, 3, 35.
- (2) Gruebele, M.; Bigwood, R. *Int. Rev. Phys. Chem.* **1998**, 17, 91.
- (3) Kellman, M. E. *Annu. Rev. Phys. Chem.* **1995**, 46, 395.
- (4) Uzer, T. *Phys. Rep.* **1991**, 199, 73.
- (5) See, for example: Pippard, A. B. *The Physics of Vibration*; Cambridge University Press: Cambridge, 1989.
- (6) Papoušek, D.; Aliev, M. R. *Molecular Vibrational-Rotational Spectra*; Elsevier: New York, 1982.
- (7) Jacobson, M. P.; Jung, C.; Taylor, H. S.; Field, R. W. *J. Chem. Phys.* **1999**, 111, 600.
- (8) Lehmann, K. K.; Ross, S. C.; Rohr, L. L. *J. Chem. Phys.* **1985**, 82, 4460.
- (9) Ishikawa, H.; Nagao, C.; Mikami, N.; Field, R. W. *J. Chem. Phys.* **1998**, 109, 492 and references therein.
- (10) Joyeux, M.; Sugny, D.; Tyng, V.; Kellman, M. E.; Ishikawa, H.; Field, R. W.; Beck, C.; Schinke, R. *J. Chem. Phys.* **2000**, 112, 4162.
- (11) Lehmann, K. K.; Scoles, G.; Pate, B. H. *Annu. Rev. Phys. Chem.* **1994**, 45, 241.
- (12) Dai, H.-L.; Field, R. W., Eds. In *Molecular Dynamics and Spectroscopy by Stimulated Emission Pumping*; World Scientific: River Edge, NJ, 1995.
- (13) Zewail A. H. *J. Phys. Chem. A* **2000**, 104, 5660.
- (14) See: Jacobson, M. P. *Spectroscopic Patterns Encode Unimolecular Dynamics*, Ph.D. Thesis, MIT, Cambridge, MA, 1999, and references therein on the extensive experimental work on C_2H_2 .

- (15) Callegari, A.; Rebstein, J.; Jost, R.; Rizzo, T. R. *J. Chem. Phys.* **1999**, *111*, 7359.
- (16) Keshavamurthy, S.; Ezra, G. S. *J. Chem. Phys.* **1997**, *107*, 156.
- (17) Jost, R.; Joyeux, M.; Skokov, S.; Bowman, J. *J. Chem. Phys.* **1999**, *111*, 6807.
- (18) Shuryak, E. V. *Sov. Phys. JETP* **1976**, *44*, 1070.
- (19) Kay, K. G. *J. Chem. Phys.* **1980**, *72*, 5955.
- (20) Sibert, E. L., III; Hynes, J. T.; Reinhardt, W. P. *J. Chem. Phys.* **1982**, *77*, 3595.
- (21) Heller, E. J.; Stechel, E. B.; Davis, M. J. *J. Chem. Phys.* **1980**, *73*, 4720.
- (22) Child, M. S.; Halonen, L. O. *Adv. Chem. Phys.* **1984**, *57*, 1.
- (23) Marcus, R. A. *Ann. N. Y. Acad. Sci.* **1980**, *357*, 169.
- (24) Ramachandran, B.; Marcus, R. A. *J. Chem. Phys.* **1981**, *74*, 1379.
- (25) Noid, D. W.; Koszykowski, M. L.; Tabor, M.; Marcus, R. A. *J. Chem. Phys.* **1980**, *72*, 6168.
- (26) Uzer, T.; Noid, D. W.; Marcus, R. A. *J. Chem. Phys.* **1983**, *79*, 4412.
- (27) Jaffé, C.; Watanabe, M. *J. Chem. Phys.* **1987**, *86*, 4499.
- (28) Lawton, R. T.; Child, M. S. *Mol. Phys.* **1981**, *44*, 709.
- (29) Farelly, D.; Uzer, T. *J. Chem. Phys.* **1986**, *85*, 308.
- (30) Noid, D. W.; Koszykowski, M. L.; Marcus, R. A. *J. Chem. Phys.* **1983**, *79*, 4412.
- (31) Ozorio de Almeida, A. M. *J. Phys. Chem.* **1984**, *88*, 6139.
- (32) Farelly, D.; Reinhardt, W. P. *J. Chem. Phys.* **1983**, *78*, 606.
- (33) Wilkinson, M. J. *Phys. A: Gen. Phys.* **1987**, *20*, 635.
- (34) Ramachandran, B.; Kay, K. G. *J. Chem. Phys.* **1993**, *99*, 3659.
- (35) Toda, M.; Ikeda, K. *J. Phys. A: Gen. Phys.* **1987**, *20*, 3833.
- (36) Berman, G. P.; Kolovsky, A. R. *Phys. Lett. A* **1987**, *125*, 188.
- (37) Lin, W. A.; Reichl, L. E. *Phys. Rev. A* **1989**, *40*, 1055.
- (38) Oxtoby, D. W.; Rice, S. A. *J. Chem. Phys.* **1976**, *65*, 1676.
- (39) Sibert, E. L., III; Reinhardt, W. P.; Hynes, J. T. *J. Chem. Phys.* **1984**, *81*, 1115.
- (40) Martens, C. C.; Davis, M. J.; Ezra, G. S. *Chem. Phys. Lett.* **1987**, *142*, 519.
- (41) Engel, Y. M.; Levine, R. D. *Chem. Phys. Lett.* **1989**, *164*, 270.
- (42) Weeks, D. E.; Levine, R. D. In *Structure and Dynamics of Non-Rigid Molecular Systems*; Kluwer: Dordrecht, The Netherlands, 1994.
- (43) Atkins, K. M.; Logan, D. E. *Phys. Lett. A* **1992**, *162*, 255.
- (44) Jaffé, C. *J. Chem. Phys.* **1988**, *89*, 3395.
- (45) Kellman, M. E.; Lynch, E. D. *J. Chem. Phys.* **1988**, *89*, 3396.
- (46) Xiao, L.; Kellman, M. E. *J. Chem. Phys.* **1990**, *90*, 6086.
- (47) Li, Z.; Xiao, L.; Kellman, M. E. *J. Chem. Phys.* **1990**, *92*, 2251.
- (48) Xiao, L.; Kellman, M. E. *J. Chem. Phys.* **1990**, *93*, 5805.
- (49) Zhilinskii, B. *Spectrochim. Acta A* **1996**, *52*, 881 and references therein.
- (50) Joyeux, M. *Chem. Phys.* **1994**, *185*, 263.
- (51) Rouben, D. C.; Ezra, G. S. *J. Chem. Phys.* **1995**, *103*, 1375.
- (52) Ezra, G. S. *J. Chem. Phys.* **1996**, *104*, 26.
- (53) Fried, L. E.; Ezra, G. S. *J. Chem. Phys.* **1987**, *86*, 6270.
- (54) Kellman, M. E. *J. Chem. Phys.* **1990**, *93*, 6630.
- (55) Rose, J. P.; Kellman, M. E. *J. Chem. Phys.* **1995**, *103*, 7255.
- (56) Lu, Z.-M.; Kellman, M. E. *Chem. Phys. Lett.* **1995**, *247*, 195.
- (57) See, for example: Simo, C., Ed. In *Hamiltonian Systems with Three or More Degrees of Freedom*; NATO-ASI series; Kluwer: Dordrecht, The Netherlands, 1999.
- (58) Husimi, K. *Proc. Phys. Math. Jpn.* **1940**, *22*, 264.
- (59) See: Keshavamurthy, S.; Ezra, G. S. In *Hamiltonian Systems with Three or More Degrees of Freedom*; Simo, C., Ed.; NATO-ASI series; Kluwer: Dordrecht, The Netherlands, 1999; p 435.
- (60) Rose, J. P.; Kellman, M. E. *J. Chem. Phys.* **1996**, *105*, 7348.
- (61) Wu, G. *Chem. Phys. Lett.* **1998**, *292*, 369.
- (62) Chirikov, B. V. *Phys. Rep.* **1979**, *52*, 263.
- (63) Graffi, S.; Paul, T.; Silverstone, H. J. *Phys. Rev. Lett.* **1987**, *59*, 255.
- (64) Davis, M. J.; Heller, E. J. *J. Chem. Phys.* **1981**, *75*, 246.
- (65) Heller, E. J. *J. Phys. Chem. A* **1999**, *103*, 10433.
- (66) Heller, E. J. *J. Phys. Chem.* **1995**, *99*, 2625.
- (67) Tomsovic, S.; Ullmo, D. *Phys. Rev. E* **1994**, *50*, 145.
- (68) Utermann, R.; Dittrich, T.; Hänggi, P. *Phys. Rev. E* **1994**, *49*, 273.
- (69) Latka, M.; Grigolini, P.; West, B. J. *Phys. Rev. A* **1994**, *50*, 1071.
- (70) Tomsovic, S., Ed. In *Tunneling in Complex Systems*; World Scientific: River Edge, NJ, 1998.
- (71) Pechukas, P. *Phys. Rev. Lett.* **1983**, *51*, 943.
- (72) Yukawa, T. *Phys. Rev. Lett.* **1985**, *54*, 1883.
- (73) Nakamura, K.; Lakshmanan, M. *Phys. Rev. Lett.* **1986**, *57*, 1661.
- (74) Calogero, F. *J. Math. Phys.* **1971**, *12*, 419.
- (75) Moser, J. *Adv. Math.* **1975**, *16*, 197.
- (76) Gibbons, J.; Hermesen, T. *Phys. D* **1984**, *11*, 337.
- (77) See: Guhr, T.; Müller-Groeling, A.; Weidenmüller, H. A. *Phys. Rep.* **1998**, *299*, 189; section 3.8 and references therein.
- (78) Pechukas, P. *Chem. Phys. Lett.* **1982**, *86*, 553.
- (79) Uzer, T.; Noid, D. W.; Marcus, R. A. *J. Chem. Phys.* **1983**, *79*, 4412.
- (80) Heisenberg, W. *Z. Phys.* **1925**, *33*, 879. Translated in *Sources of Quantum Mechanics*; Van der Waerden, B. L., Ed.; Dover: Minneola, NY, 1967.
- (81) Lichtenberg, A. J.; Lieberman, M. A. *Regular and Stochastic Motion*; Springer-Verlag: New York, 1983.
- (82) Keshavamurthy, S. *Ind. J. Chem.* **2000**, *39A*, 307.
- (83) Ravishankar, V. Private communication.
- (84) Takami, T.; Hasegawa, H. *Phys. Rev. Lett.* **1992**, *68*, 419.
- (85) Simons, B. D.; Altshuler, B. L. *Phys. Rev. Lett.* **1993**, *70*, 4063.
- (86) Fyodorov, Y. V. *Phys. Rev. Lett.* **1994**, *73*, 2688.
- (87) Zakrzewski, J.; Delande, D. *Phys. Rev. E* **1993**, *47*, 1650.
- (88) Guarneri, I.; Zyczkowski, K.; Zakrzewski, J.; Molinari, L.; Casati, G. *Phys. Rev. E* **1995**, *52*, 2220.
- (89) Sano, M. *Phys. Rev. E* **1996**, *54*, 3591.
- (90) Kuntsman, P.; Zyczkowski, K.; Zakrzewski, J. *Phys. Rev. E* **1997**, *55*, 2446.
- (91) Lakshminarayan, A.; Cerruti, N. R.; Tomsovic, S. *Phys. Rev. E* **1999**, *60*, 3992.
- (92) Tomsovic, S. *Phys. Rev. Lett.* **1996**, *77*, 4158.
- (93) Cerruti, N. R.; Lakshminarayan, A.; Lefebvre, J. H.; Tomsovic, S. *Phys. Rev. E* **2001**, *63*, 016208.